Molecular Biology of the Cell
Vol. 19, 4776–4784, November 2008

Activation of the MAPK Module from Different Spatial Locations Generates Distinct System Outputs

Kerry Inder,* Angus Harding,† Sarah J. Plowman,*‡ Mark R. Philips,§ Robert G. Parton,*‖ and John F. Hancock*‡

*Institute for Molecular Bioscience, University of Queensland, Brisbane 4072, Australia; †Queensland Brain Institute, University of Queensland, Brisbane 4072, Australia; §New York University School of Medicine, New York, NY 10016; and ‖Centre for Microscopy and Microanalysis, University of Queensland, Brisbane 4072, Australia

Submitted April 21, 2008; Revised July 25, 2008; Accepted August 28, 2008
Monitoring Editor: J. Silvio Gutkind

The Ras/Raf/MEK/ERK (MAPK) pathway directs multiple cell fate decisions within a single cell. How different system outputs are generated is unknown. Here we explore whether activating the MAPK module from different membrane environments can rewire system output. We identify two classes of nanoscale environment within the plasma membrane. The first, which corresponds to nanoclusters occupied by GTP-loaded H-, N- or K-Ras, supports Raf activation and amplifies low Raf kinase input to generate a digital ERKpp output. The second class, which corresponds to nanoclusters occupied by GDP-loaded Ras, cannot activate Raf and therefore does not activate the MAPK module, illustrating how lateral segregation on plasma membrane influences signal output. The MAPK module is activated at the Golgi, but in striking contrast to the plasma membrane, ERKpp output is analog. Different modes of Raf activation precisely correlate with these different ERKpp system outputs. Intriguingly, the Golgi contains two distinct membrane environments that generate ERKpp, but only one is competent to drive PC12 cell differentiation. The MAPK module is not activated from the ER. Taken together these data clearly demonstrate that the different nanoscale environments available to Ras generate distinct circuit configurations for the MAPK module, bestowing cells with a simple mechanism to generate multiple system outputs from a single cascade.

INTRODUCTION

The small G-protein Ras regulates cell proliferation, differentiation and survival by transmitting signals from activated receptors on the plasma membrane. Ras operates as a membrane-bound molecular switch, cycling between active GTP-bound and inactive-GDP–bound conformations. One of the core signaling pathways activated by Ras is the mitogen-activated protein kinase cascade (MAPK) comprised of Raf, MEK, and ERK (Marshall, 1996). The Ras–Raf interaction is the crucial first step in Raf activation; however, Raf activation is a complex process that involves Ras binding, interaction with lipids, de-phosphorylation of inhibitory residues and phosphorylation of activating residues, and changes in protein–protein interactions (Morrison and Cutler, 1997; Dhillon and Kolch, 2002; McKay and Morrison, 2007). Active Raf phosphorylates two serine residues within the MEK activation loop. Once activated, MEK phosphorylates and activates ERK, allowing the MAPK module to regulate a diverse portfolio of cellular functions. Understanding how the MAPK pathway processes multiple inputs to generate different and often opposing biological outputs remains a central question in signal transduction (Santos *et al.*, 2007).

The solution to this conundrum may lie in the ability of Ras proteins to signal from different membrane environments in vivo. The classical Ras isoforms, H-Ras, K-Ras, and N-Ras, are tethered to the inner leaflet of the plasma membrane by carboxy-terminal lipid anchors (Hancock *et al.*, 1989, 1990). The Ras isoforms are highly conserved except for significant sequence divergence in the carboxy-terminal 25 amino acids of the hypervariable region (HVR). The plasma membrane itself is a complex mosaic of dynamically distributed lipids and proteins that inflicts nonrandom distribution of signaling proteins into different types of transient nanodomains. H-Ras, K-Ras, and N-Ras each assemble into distinct, transient nanoclusters driven by interactions between the membrane anchor, flanking protein sequences, and lipids and proteins of the plasma membrane (Hancock and Parton, 2005; Abankwa *et al.*, 2008). This lateral segregation is also regulated by Ras activation, because GTP-loaded H- and N-Ras proteins form nanoclusters that are spatially and structurally distinct from those formed by the cognate GDP-loaded proteins (Prior *et al.*, 2001, 2003; Jaumot *et al.*, 2002; Plowman *et al.*, 2005; Abankwa *et al.*, 2008). Ras nanoclusters are the sites of effector recruitment and activation (Hibino *et al.*, 2003; Murakoshi *et al.*, 2004; Tian *et al.*, 2007; Plowman *et al.*, 2008). Importantly, individual K-Ras-GTP nanoclusters function as highly sensitive digital switches, translating graded Raf kinase inputs into fixed ERKpp signal outputs (Harding *et al.*, 2005; Tian *et al.*, 2007; Harding and Hancock, 2008a). The signal outputs of N- and H-Ras nanoclusters at the plasma membrane are unknown,

This article was published online ahead of print in *MBC in Press* (http://www.molbiolcell.org/cgi/doi/10.1091/mbc.E08–04–0407) on September 10, 2008.

‡ Present address: Department of Integrative Biology and Pharmacology, University of Texas Health Science Center, Houston, TX 77030.

Address correspondence to: John F. Hancock (John.F.Hancock@uth.tmc.edu).

but in theory could be quite different from that of K-Ras nanoclusters, allowing the generation of multiple ERKpp outputs from the plasma membrane.

In addition to the plasma membrane, Ras proteins inhabit and signal from a wide range of internal membrane environments including the endoplasmic reticulum (ER) and Golgi (Chiu *et al.*, 2002; Roy *et al.*, 2002; Tohgo *et al.*, 2002; Perez de Castro *et al.*, 2004; Matallanas *et al.*, 2006). Ras activation on the Golgi does not require endocytosis or vesicular transport (Chiu *et al.*, 2002) and is mediated by Src-dependent signaling through PLCγ1 and RasGPR1, separate from the Grb2/SOS pathway that activates signaling from the plasma membrane (Bivona *et al.*, 2003). Ras activation kinetics differ between the Golgi and the plasma membrane, with activation of Golgi-localized Ras being delayed but sustained and with the plasma membrane being more rapid and transient (Chiu *et al.*, 2002; Rocks *et al.*, 2005). The kinetics of Golgi signaling also varies between cell types, with Golgi signaling in lymphocytes being several fold faster than in fibroblasts (Bivona *et al.*, 2003). Interestingly, low-grade stimulation of lymphocytes specifically activates N-Ras on the Golgi (Perez de Castro *et al.*, 2004). Moreover, positive selection in lymphocytes induces recruitment and activation of RasGRP1 and Ras at the Golgi, whereas negative selection targets plasma membrane signaling (Daniels *et al.*, 2006). Together these studies indicate that fundamentally different biological outcomes from the MAPK pathway may be generated from different subcellular compartments; however, the biochemistry and system outputs that underpin these biological outcomes are unknown.

MATERIALS AND METHODS

Plasmids

CTK, tK, CTH, tH, CTN, tN, KDELR, and IBVM-1 targeting motifs were cloned into GFP-Raf-1 construct. Mutations were introduced by PCR mutagenesis.

Antibodies and Reagents

Antibody against Ras and Raf-1 were purchased from BD Transduction Laboratories (Lexington, KY). Raf-1 pS338, MEKpp, and ERKpp antibodies were from Cell Signaling Technology (Beverly, MA). ERK2 antibody was purchased from Santa Cruz Biotechnology (Santa Cruz, CA).

Cell Culture

Baby hamster kidney (BHK) cells were grown and maintained in HEPES-buffered Dulbecco's modified Eagle's Medium containing 10% serum supreme. NIH3T3 and COS-1 cells were maintained in 10% fetal bovine serum. Cells were transfected using Lipofectamine 2000 (Invitrogen, Carlsbad, CA) according to the manufacturer's instructions and harvested after 24 h. PC-12 cells were cultured in Dulbecco's modified Eagle's Medium supplemented with 5% horse serum and 10% calf serum and transfected on coverslips using Lipofectamine 2000. Cells were grown for 72 h and analyzed for differentiation.

Immunofluorescence

Cells transfected onto coverslips were fixed in 4% paraformaldehyde after 24 h. The coverslips were quenched with 50 mM ammonium chloride and then permeabilized and blocked in 0.1% Triton, 3% BSA in phosphate-buffered saline for 30 min. Anti-protein disulfide isomerase (PDI) or anti-GM-130 was incubated on coverslips for 1 h, and anti-pERK was incubated overnight at 4°C, followed by secondary antibody, either mouse or rabbit-Cy3, for another hour. Coverslips were stained with DAPI for 5 min and mounted in Mowiol for confocal microscopy. Quantitative fluorescent microscopy was performed as previously described (Harding *et al.*, 2005).

Western Blotting

Cytosolic (S100) and membrane (P100) fractions prepared by 100,000 × *g* ultracentrifugation, or whole cell lysates, normalized for protein content, were resolved on SDS-PAGE gels and transferred to PVDF using semidry transfer. The membranes were probed with anti-Raf-1, anti-Ras, anti-Raf-1 p338, anti-pMEK, anti-pERK, or anti-ERK2 antibodies, developed using horseradish peroxidase–conjugated secondary antibodies and enhanced chemi-luminescence and imaged on a LumiImager (Roche Molecular Biochemicals, Indianapolis, IN).

Raf-1 Kinase Assay

BHK cells were subjected to hypotonic lysis, and a P100 fraction was prepared from postnuclear supernatants as described previously (Hancock *et al.*, 1989). P100 aliquots were normalized for protein content and assayed for Raf-1 activity by using a coupled MEK/ERK assay (Roy *et al.*, 1997).

Electron Microscopy

Apical plasma membrane sheets were prepared, fixed with 4% PFA, 0.1% glutaraldehyde, and labeled with affinity-purified anti-green fluorescent protein (GFP) antibodies conjugated directly to 5-nm gold as described previously (Prior *et al.*, 2003; Plowman *et al.*, 2005). Digital images of the immunogold-labeled plasma membrane sheets were taken at 100,000× magnification in an electron microscope (Jeol 1011, Peabody, MA). Intact 1-μm^2 areas of the plasma membrane sheet were identified using Image J (http://rsb.info.nih.gov/ij/) and the (x,y) coordinates of the gold particles determined as described (Prior *et al.*, 2003; Plowman *et al.*, 2005).

RESULTS

Raf-1 Targeted to the Plasma Membrane Functions as a Digital Switch

To formally address whether different nanoscale membrane environments reconfigure the MAPK pathway, we compared the ERKpp outputs from the MAPK module activated from specific cellular locations that have been reported to operate as MAPK-signaling platforms. We first examined signal outputs from all types of plasma membrane Ras nanocluster. To this end we cloned the complete carboxy-terminal hypervariable region of H-Ras, N-Ras (amino acids 166–189), and K-Ras (166–188) onto the C-terminus of GFP-Raf-1, to generate Raf-CTH, Raf-CTN, and Raf-CTK, respectively. These Ras C-terminal sequences direct the Raf proteins to plasma membrane nanoclusters that colocalize with the cognate GTP-loaded Ras isoforms (Supplemental Figure S1; Prior *et al.*, 2003). In addition we cloned the minimal membrane anchors of each Ras isoform (amino acids 180–189 for H-Ras and N-Ras and 175–188 for K-Ras) onto the C-terminus of GFP-Raf-1, to generate Raf-tH, Raf-tN, and Raf-tK. The minimal anchor of H-Ras, targets GFP-tH to H-rasGDP nanoclusters, whereas the minimal anchor of K-Ras targets GFP-tK to K-Ras-GTP nanoclusters (Prior *et al.*, 2003). The GFP-Raf constructs were transiently transfected into BHK cells and their subcellular localizations observed by fluorescent microscopy. Raf-CTK, -tK, -CTH, -tH, -CTN, and -tN were localized extensively to the plasma membrane, although Raf-tH and Raf-tN also displayed a prominent Golgi pool (Supplemental Figure S2). No ER localization was evident for any of these Raf constructs (Supplemental Figure S2). The subcellular localization of this set of Ras anchors therefore exactly match previous characterizations (Choy *et al.*, 1999; Apolloni *et al.*, 2000; Laude and Prior, 2008). To quantify and evaluate plasma membrane association intact plasma membrane sheets were prepared from BHK cells ectopically expressing each targeted GFP-Raf protein and labeled with immunogold conjugated anti-GFP antibody. The extent of immunogold labeling did not differ significantly among any of the targeted Raf proteins, indicating that all were retained at the plasma membrane with equal efficiency (Supplemental Figure S1), a result consistent with biochemical analysis of P100 association (Supplemental Figure S3). Spatial analysis of the immunogold point patterns further confirmed that the GFP-Raf proteins were organized into plasma membrane nanoclusters (Supplemental Figure S1).

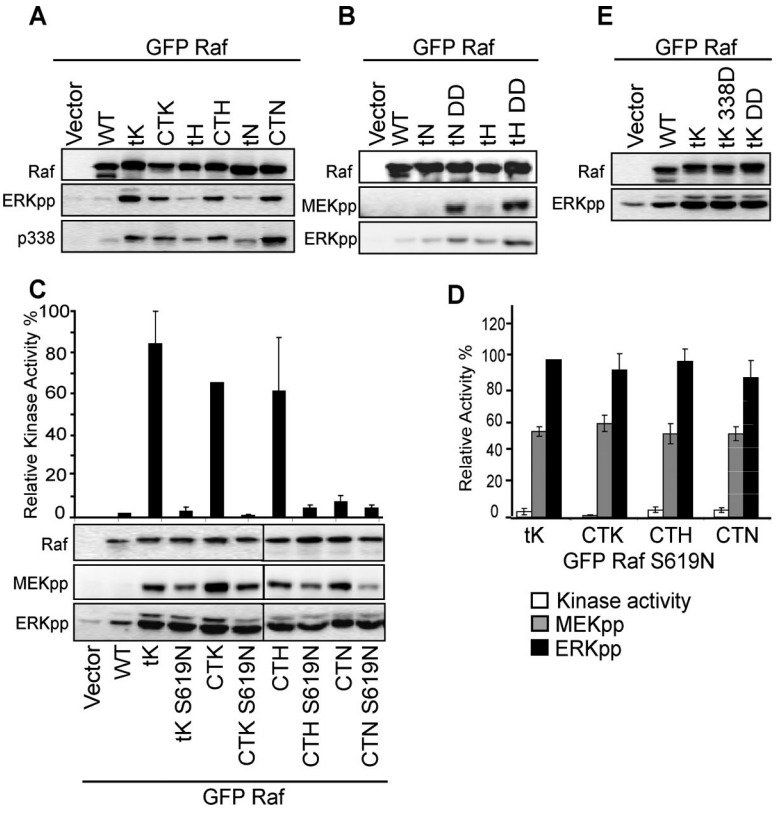

Figure 1. Raf-1 targeted to the plasma membrane functions as a digital switch. (A) Raf-CTK, Raf-tK, Raf-CTH, Raf-tN, Raf-CTN, and Raf-tH were transiently expressed in BHK cells and cell lysates prepared after 3 h of serum starvation. Empty vector and wild-type Raf-1 (WT) were used as controls. The Raf-1 Western blot shows equivalent expression of the Raf constructs. Activation of Raf-1 and ERK was assayed with phospho-specific antibodies: pS338-Raf-1 and ERKpp, respectively. (B) BHK cells were transfected with empty vector, wild-type Raf-1 (WT), Raf-tH, Raf-tN, and the cognate constitutively active constructs (DD). Cells were then serum-starved. The Raf-1 Western blot shows equivalent expression of the Raf constructs. Activation of MEK and ERK was assayed with phospho-specific antibodies: MEKpp and ERKpp, respectively. (C) Membrane fractions (P100) prepared from serum-starved BHK cells transiently expressing wild-type Raf-1 (WT), Raf-tK, Raf-CTK, Raf-CTH, or Raf-CTN with and without a kinase mutation (S619N) or from vector transfected control cells were assayed for Raf-1 kinase activity in a coupled MEK/ERK assay. The graph shows mean activity ± SEM (n = 3). Corresponding whole cell lysates were immunoblotted for Raf-1 (to show equivalent Raf expression), MEKpp, and ERKpp. (D) A comparison of Raf kinase activity, MEK activity (MEKpp), and ERK activity (ERKpp) of the kinase reduced (S619N) constructs expressed relative to the cognate wild-type Raf-1 construct (mean ± SEM, n = 3). The results show that each S619N mutant has <5% Raf catalytic activity, ~50% MEK activity, and 100% ERK activity compared with the wild-type control levels, respectively. Indicative of switch-like signal transmission. (E) BHK cells expressing empty vector, wild-type Raf-1 (WT), Raf-tK, and constitutively active Raf-tK-338D and Raf-tK-DD were serum-starved for 3 h and assayed with Raf-1 and ERKpp antibodies.

We measured activation of the MAPK cascade from each different type of Ras nanocluster. Raf targeted to -CTK, -tK, -CTH, and -CTN nanoclusters robustly activated ERK, whereas Raf-1 directed to -tH and -tN clusters generated very low levels of activated ERKpp (Figure 1A). To explore the basis of these differences we assessed the degree of Raf activation using an antibody specific to Raf phosphorylated on S338, one of the key Raf activation events (Diaz *et al.*, 1997). We observed a high degree of phosphorylation of S338 on Raf-tK, -CTK, -CTH, and -CTN, but low levels on Raf-tH and Raf-tN. These results suggest that active Ras nanoclusters are competent to activate Raf, whereas nanoclusters that correspond to inactive Ras are not. In all cases the expression level of the targeted Raf constructs was kept close to those of endogenous Raf, and in no experiment was the expression level of membrane-associated Raf more than two- to threefold greater than that of endogenous Raf (Supplemental Figure S3). In consequence the maximum levels of ERKpp generated, for example, by Raf-tK, were of a similar magnitude to that achieved by stimulating cells with epidermal growth factor (EGF) or ectopically expressing oncogenic mutant K-ras (Supplemental Figure S3).

To determine if -tH and -tN nanoclusters are capable of MEK and ERK recruitment and activation, Raf-tH and Raf-tN were rendered constitutively active by the double mutation Y340D,Y341D (DD). Analysis of MAPK output (Figure 1B) showed a significant increase in MEKpp and ERKpp levels from constitutively active Raf-tH-DD and Raf-tN-DD compared with the wild-type Raf-tH and Raf-tN. This shows Raf can activate the MAPK module from -tH and -tN nanoclusters, but only if the Raf kinase domain is preactivated. Taken together these data provide evidence for two classes of nanocluster at the plasma membrane. The first class supports Raf activation and activates the MAPK module, whereas the second class does not support Raf activation and therefore does not activate the MAP kinase module.

We have previously established that K-Ras nanoclusters function as high-gain amplifiers of the MAP kinase module (Tian *et al.*, 2007). We next asked whether different Ras nanoclusters reconfigure the MAPK module to give different outputs. We directly measured Raf kinase activity in a coupled MEK/ERK kinase assay. Raf-tK, Raf-CTK, and Raf-CTH possessed very high kinase activity, whereas Raf-CTN exhibited 6–10-fold lower kinase activity (Figure 1C), and no measurable kinase activity was associated with Raf-tH and Raf-tN (data not shown). In addition, we introduced a well-characterized point mutation, S619N (Harding *et al.*, 2003, 2005; Tian *et al.*, 2007) into the kinase domain of Raf-tK, Raf-CTK, Raf-CTH, and Raf-CTN. The S619N mutation reduced Raf kinase activity of all of the nanoclustered Raf proteins to <5% of wild-type (Figure 1, C and D). Each S619N mutant Raf-tK, Raf-CTK, Raf-CTH, and Raf-CTN with <5% catalytic function generated active MEKpp levels that were ~50% of those generated by the cognate wild-type targeted Raf with full catalytic activity. In turn, the reduced levels of MEKpp stimulated the same maximum ERKpp response as the wild-type control levels.

To verify that the ERKpp response from plasma membrane nanoclusters cannot be further increased, we introduced point mutations into Raf-tK at key Raf activation sites, S338 and Y340/Y341, to render these sites constitutively active (GFP-Raf-tK S338D and GFP-Raf-tK YY340/341DD). Analysis of the ERKpp levels revealed that these point mutations did not increase signal output when compared with

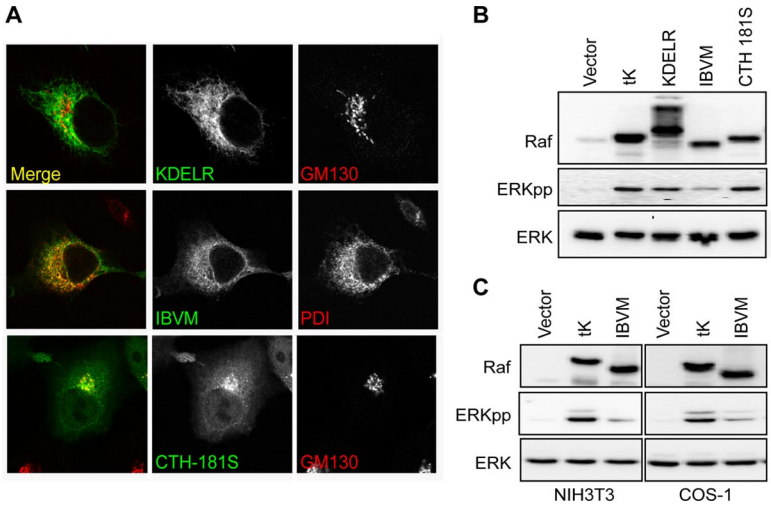

Figure 2. Raf-1 signaling from the Golgi. (A) Endomembrane-targeted Raf-1 constructs were transiently expressed in BHK cells and colocalized with organelle markers. Raf-KDELR and Raf-IBVM colocalize with GM130 (Golgi marker) and PD1 (ER marker), respectively. Raf-KDELR also shows some degree of ER localization. Raf-CTH-181S localizes exclusively with GM130 to the Golgi. (B) Raf-KDELR, Raf-IBVM, and Raf-CTH-181S were transfected into BHK cells and serum-starved for 3 h. Empty vector and Raf-tK were used as negative and positive controls for ERK activation, respectively. Activation of ERK was assayed in immunoblots of whole cell lysates with phospho-specific antibody ERKpp, and total ERK levels were blotted with anti-ERK 2. (C) ERK activation was assessed from Raf-IBVM expressed in NIH3T3 and COS-1 cells. Empty vector and Raf-tK were used as negative and positive controls. Western blots shows equal loading with ERK antibody and ERK activation with ERKpp phospho-specific antibody.

Raf-tK (Figure 1D), confirming that the signal output from active Ras nanoclusters is at a maximum level. Taken together, these results show that all plasma membrane nanoclusters that activate Raf process variations in Raf input levels and convert them into a maximal ERKpp signal output, including the N-Ras (-CTN) nanocluster, which has a reduced capacity for Raf-1 activation. Thus all Ras nanoclusters at the plasma membrane have the same system output, functioning as high-gain amplifiers to generate maximal ERKpp output irrespective of Raf kinase input.

Signaling from the Golgi Generates Analog Signal Output

We next explored MAPK signal outputs from the endomembrane. Raf was targeted to the Golgi using a KDEL receptor-2 (KDELR) sequence. Raf-KDELR showed significant Golgi and ER staining (Figure 2A), reflecting shuttling between the ER and Golgi. As an alternative approach to target Raf specifically to the ER, we used the cytoplasmic tail of the first transmembrane domain of the avian infectious bronchitis virus M protein (Raf-IBVM), which harbors an ER-retention signal. Exclusive ER-localization of Raf-IBVM was verified by colocalization with PDI, an ER marker (Figure 2A). We expressed the endomembrane Raf constructs in BHK cells to identify which compartments would elicit MAPK signaling. Raf-KDELR induced robust activation of ERK, whereas Raf-IBVM did not, suggesting that activation of the MAPK module occurs from the Golgi but not the ER (Figure 2B). To confirm this observation, we generated a precise Golgi localized construct by introducing a cysteine-to-serine substitution at residue 181 of the Raf-CTH anchor (Raf-CTH-181S). A similar substitution confines H-RasC181S almost completely to the Golgi (Goodwin *et al.*, 2005; Rocks *et al.*, 2005; Roy *et al.*, 2005). Exclusive Golgi localization of Raf-CTH-181S was confirmed by immunofluorescent microscopy and colocalization with the Golgi marker GM130 (Figure 2A). Expression of Raf-CTH-181S in BHK cells activated ERK phosphorylation (Figure 2B). The ER-localized Raf-IBVM construct was also unable to activate ERK in NIH3T3 and COS-1 cells (Figure 2C). We therefore conclude that the MAPK module can be efficiently activated from the Golgi, but not from the ER.

To assess whether the Golgi amplifies low Raf input to produce a digital output we modified the kinase activity of Raf-KDELR and Raf-CTH-181S. We constructed kinase-reduced (Raf-KDELR-S619N), constitutively active (Y340D,Y341D; Raf-KDELR-DD), and a construct containing both mutations (Raf-KDELR-S619N-DD). The Raf-CTH-181S construct was similarly engineered to kinase reduced and constitutively active forms using S619N and Y340D,Y341D mutations, respectively. The Raf proteins were expressed in BHK cells, and MAPK signaling was analyzed (Figure 3A). The results show that expression of the kinase-reduced Raf-KDELR and -CTH-181S in BHK cells reduced activation of MEK and ERK compared with wild-type, whereas expression of constitutively active Raf-KDELR and -CTH-181S increased MEK and ERK activation. Raf-KDELR with both sets of mutations (Raf-KDELR-S619N-DD) showed no change from the wild type. These results show that in striking contrast to the plasma membrane, MAPK signaling from the Golgi generates a graded ERKpp output and confirm the hypothesis that different spatial locations do indeed rewire the MAPK module to generate different system outputs in vivo.

Given the central role of Raf phosphorylation at the plasma membrane, we next examined the phosphorylation status of Golgi-localized Raf-1 in an effort to understand how a graded output is generated from this location. Interestingly, we could not detect S338 phosphorylation on Raf-KDELR or Raf-KDELR-DD despite the ability of these Raf proteins to robustly activate ERK (Figure 3B). In fact Raf-KDELR had lower levels of phosphorylated S338 than wild-type Raf-1 that is predominantly cytosolic and inactive. Thus Golgi Raf-1 appears to be exempt from this key activating phosphorylation event. To verify this observation, we introduced S338A or S338D mutations into Raf-KDELR and Raf-CTH-181S to block or mimic phosphorylation of S338, respectively, and analyzed MAPK signal output. Neither S338A, nor S338D mutations had any effect on the level of ERK activation generated by Raf-KDELR or Raf-CTH-181S (Figure 3, A and B). In combination these results show that S338 phosphorylation is not required for activation of Raf from the Golgi, despite being an important activation event for plasma membrane recruited Raf-1.

Biological Outputs from ERKpp Are Also Spatially Regulated

Finally we sought to determine whether activating the MAPK module from different spatial compartments produced correspondingly divergent biological outcomes. To this end we used the established assay of PC-12 differentiation to score biological output of the targeted Raf con-

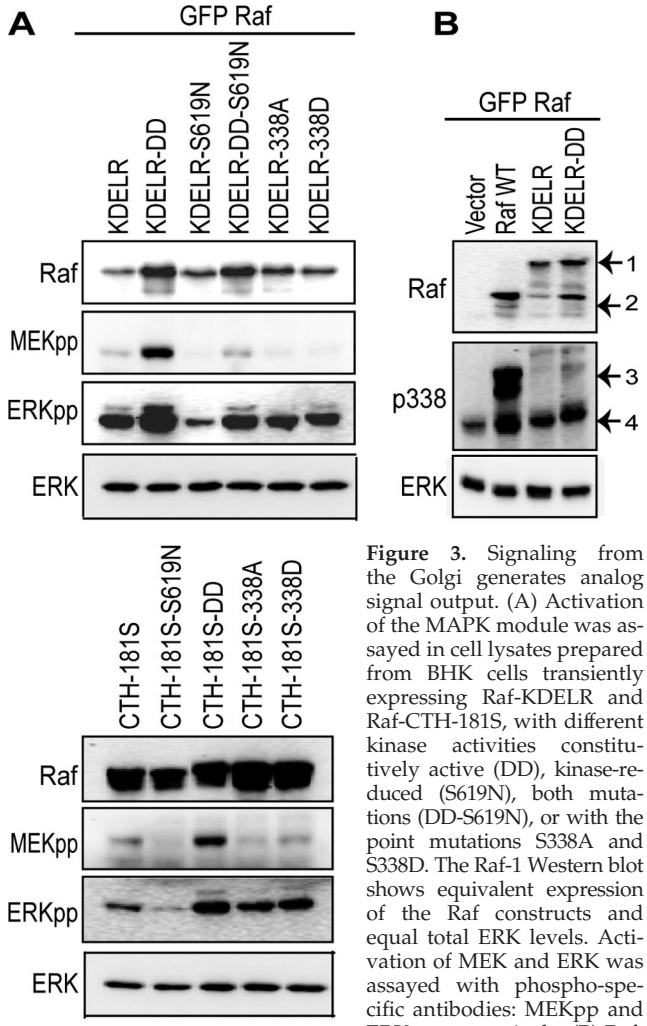

Figure 3. Signaling from the Golgi generates analog signal output. (A) Activation of the MAPK module was assayed in cell lysates prepared from BHK cells transiently expressing Raf-KDELR and Raf-CTH-181S, with different kinase activities constitutively active (DD), kinase-reduced (S619N), both mutations (DD-S619N), or with the point mutations S338A and S338D. The Raf-1 Western blot shows equivalent expression of the Raf constructs and equal total ERK levels. Activation of MEK and ERK was assayed with phospho-specific antibodies: MEKpp and ERKpp, respectively. (B) Raf-KDELR and constitutively active Raf-KDELR-DD transiently expressed in BHK cells show very low levels of Raf S338 phosphorylation detected by immunoblotting with pS338-Raf-1 antisera. Lysates prepared from empty vector and wild-type Raf-1 (WT)-transfected cells are included as negative controls. Equal protein loading is shown by total ERK levels. Arrow 1 points to Raf-KDELR protein, whereas arrow 2 is the degradation product. Arrow 3 corresponds to phosphorylation of the expressed GFP-Raf proteins, and arrow 4 is the phosphorylation of endogenous Raf.

structs. Pronounced differences were observed between the different cellular locations of Raf (Figure 4A). Raf directed to Ras plasma membrane nanoclusters that induced ERK activation (Raf-tK, -CTK, -CTH, and -CTN) also stimulated equivalent PC-12 differentiation, whereas Raf-tH and -tN did not. This is entirely consistent with our finding that nanoclusters corresponding to all active Ras isoforms generate maximal ERKpp output, whereas those corresponding to inactive Ras cannot activate the MAPK module. Golgi specific Raf-CTH-181S also induced PC-12 differentiation, although to lower levels than plasma membrane Raf, consistent with the activation of the MAPK module from the Golgi observed above. In striking contrast, Golgi localized Raf-KDELR induced limited differentiation despite an equally robust ERK activation.

Cell proliferation and differentiation is driven by translocation of phosphorylated ERK to the nucleus (Traverse *et al.*, 1992; Robinson *et al.*, 1998; Brunet *et al.*, 1999). We analyzed the level of nuclear ERKpp in single cells expressing relatively equal levels of Raf-tK, Raf-KDELR, and Raf-CTH-181S and the corresponding mutants, S619N (kinase reduced) and DD (constitutively active; Figure 4, B and C). The majority of Raf-tK–expressing cells generated maximal levels of nuclear ERKpp. Manipulating the kinase activity of Raf-tK had no significant effect on the nuclear ERKpp profile in that single cells expressing Raf-tK S619N and Raf-tK DD had levels of nuclear ERKpp similar to that of control Raf-tK cells. This result is consistent with Ras plasma membrane nanoclusters functioning as digital switches that generate maximal ERK output irrespective of Raf input. In contrast the modal and mean nuclear ERKpp levels of cells expressing Golgi-localized Raf-CTH-181S or Raf-KDELR correlated closely with Raf kinase activity. The single-cell nuclear ERKpp profile of Raf-CTH-181S or Raf-KDELR shifted to higher values as Raf kinase activity increased in the order S619N $<$ WT $<$ DD. These data provide further support for graded or analog signaling from the MAPK module when it is localized to the Golgi complex.

Analog Signal Output from the Golgi in Response to EGF Stimulation

Finally we explored whether endogenous activation of the MAPK module on the Golgi in response to EGF stimulation was also analog. To compare and contrast MAPK activation from the plasma membrane and Golgi, we took advantage of previous work that characterized different activation kinetics for the two compartments. EGF stimulation drives RBD recruitment almost exclusively to the plasma membrane at early time points (2–10 min) and to the Golgi at later time points (40 min; Chiu *et al.*, 2002). Therefore, we compared endogenous signaling dynamics from the plasma membrane and Golgi, respectively, by measuring MAPK activation after 2 and 40 min of EGF stimulation. Figure 5 shows the ERKpp levels in serum-starved BHK cells stimulated with a range of EGF concentrations for the two time points. The maximum levels of ERKpp generated from the Golgi and plasma membrane in response to EGF were equal, but were achieved at 3 versus 15 ng/ml EGF, respectively (Figure 5). Most interestingly however, the 2- and 40-min ERKpp activation profiles are very different. In accordance with previously published data, the generation of ERKpp from the plasma membrane (2-min profile) exhibits a linear relationship with the EGF concentration, a consequence of switch-like signaling within Ras nanoclusters (Tian *et al.*, 2007). In contrast, ERKpp activation from Golgi (40-min profile) at nonsaturating doses of EGF is strikingly nonlinear. Importantly, the shape of the Golgi activation profile observed in Figure 5 is as predicted for graded or analog activation of the MAPK module within Ras nanoclusters (Tian *et al.*, 2007; Harding and Hancock, 2008a,b).

DISCUSSION

There is increasing evidence that specificity in MAPK signaling is achieved through spatial and temporal regulation. However, it is unclear how subcellular localization might regulate properties such as signal duration and signal intensity. To address this, we constructed Raf-1 proteins targeted to specific cellular locations and distinct plasma membrane nanodomains that have been reported to operate as MAPK signaling platforms. We observed striking differences in the ability of different types of Ras nanocluster to drive MAPK activation, providing further evidence for the importance of lateral segregation of signaling cascades on the plasma

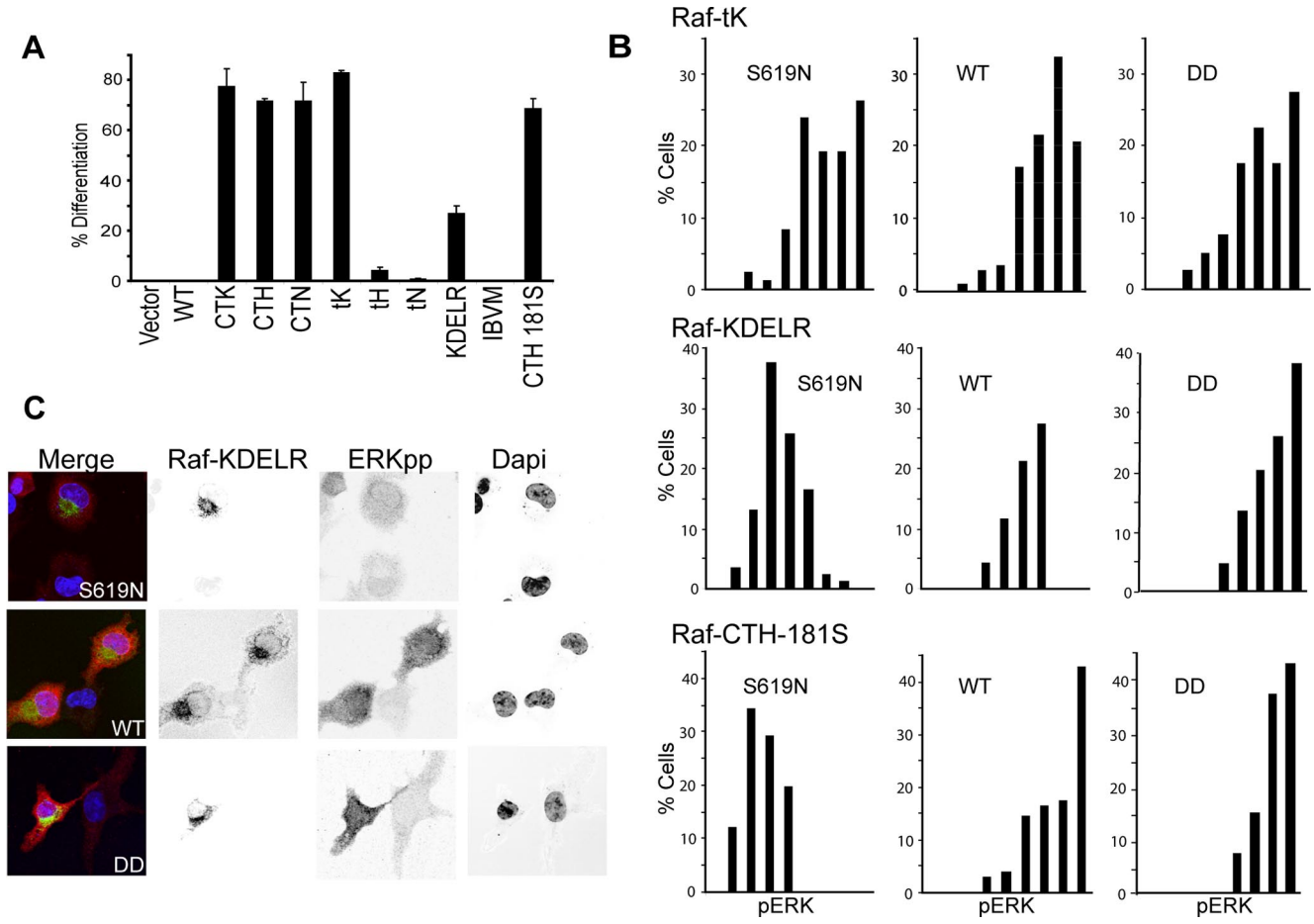

Figure 4. Biological outputs from ERKpp are spatially regulated. (A) PC-12 cells transfected with the indicated constructs were assayed for differentiation after 3 d. The graph shows the mean percentage (± SEM, n = 100) of transfected (GFP positive) cells with neurite outgrowth equal to or more than twice the cell body size at 72 h. (B) Serum-starved cells expressing relatively equal Raf-tK, Raf-KDELR, Raf-CTH-181S, and respective S619N and DD mutants were immunostained for pERK. Nuclear pERK was quantitated in single cells (n ≥100) and is displayed in nine bins in the frequency histogram. (C) Representative cells show expression of GFP-Raf-KDELR (WT), GFP-Raf-KDELR-S619N, and GFP-Raf-KDELR-DD, with ERKpp levels detected by Cy3 secondary antibody; DAPI stain of the nucleus; and merged images. Each image displays transfected and nontransfected cells for comparison.

membrane. We also found that the system output from the MAPK module is fundamentally different when activated on plasma membrane or endomembranes. This illustrates that the nanoscale heterogeneity within membrane environments can effectively rewire MAPK signaling dynamics to generate multiple system outputs.

Activation of the MAPK module from the plasma membrane revealed that not all Ras nanoclusters support Raf-1 activation. Robust activation of ERKpp occurred from -CTK, -tK, -CTH, and -CTN nanoclusters, but not from -tH and -tN nanoclusters. These data provide evidence for two classes of nanocluster at the plasma membrane. The first class corresponds to active Ras, supports Raf activation, and activates the MAPK module. The second class corresponds to inactive Ras, does not support Raf activation, and does not activate the MAP kinase module. Importantly, the ability of plasma membrane nanoclusters to activate the MAPK module is entirely dependent on their ability to activate Raf, because targeting constitutively active Raf to the -tH and -tN "null" nanoclusters rescued their ability to activate ERK.

Interestingly all plasma membrane nanoclusters that activate Raf have the same system output, functioning as high-gain amplifiers to generate maximal system output. This

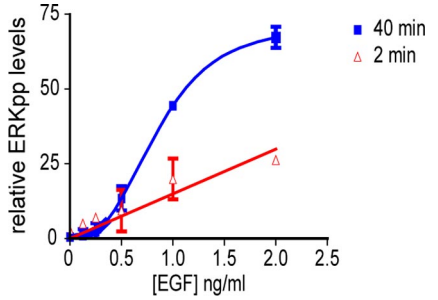

Figure 5. Different endogenous signaling dynamics are observed from the plasma membrane versus the Golgi. BHK cells were serum-starved for 3 h and stimulated with EGF at the following concentrations: 0, 0.125, 0.25, 0.5, 1, 2, and 15 ng/ml for 2 min (to assay plasma membrane ERKpp output) and 40 min (to assay Golgi ERKpp output). ERKpp was quantified from Western blots and graphed (mean ± SEM, n = 3). ERKpp values are expressed as a % of the maximal value observed at 2 min with 15 ng/ml EGF. The Golgi ERKpp response rapidly plateaus after 3 ng/ml EGF as shown in the figure, whereas the plasma membrane response continues to increase linearly as shown both here and previously (Tian *et al.*, 2007).

implies that scaffolding the MAPK module in plasma membrane nanoclusters results in a low activation threshold such that low levels of Raf kinase input generate maximal ERKpp signal output. The composition of activated N-Ras nanoclusters, however, was not optimal for Raf-1 activation. This may be related to N-Ras-GTP nanoclusters being cholesterol-dependent domains (Roy *et al.*, 2005), whereas H-Ras-GTP and K-Ras-GTP nanoclusters are cholesterol-independent domains. Previous work has shown that mistargeting H-Ras-GTP to cholesterol-dependent nanoclusters abrogates signal transmission to Raf-1 (Prior *et al.*, 2001), although the molecular basis of this effect remains unclear. Nevertheless -CTN nanoclusters still induce maximal ERK activation because of switch-like MAPK signaling.

In striking contrast to the plasma membrane, MAPK signaling from the Golgi generates a graded ERK output, indicating that different spatial locations do indeed rewire the MAPK module to generate different system outputs in vivo. Moreover, we successfully converted the ERKpp system output of Raf-CTH from digital to analog simply by redirecting it to the Golgi. This result clearly demonstrates that the nanoscale membrane environment is able to dictate signaling properties such as the activation threshold rather than these being inherent properties of the signaling complex. Our results further show that S338 phosphorylation is associated with Raf activation at the plasma membrane, but is not relevant for Raf activation or MAPK signaling from the Golgi. These different modes of Raf activation in turn precisely correlate with different ERK outputs, implicating Raf as a key control point in determining system output from the MAPK module.

It seems likely that the different mechanisms of Raf-1 activation on the Golgi and plasma membrane are a consequence of spatially constrained kinases, or other coactivators. In support of this conclusion a recent study showed that the plasma membrane scaffold KSR not only delivers MEK and ERK to Raf, but also the active haloenzyme CK2, required for Raf phosphorylation at S338 (Ritt *et al.*, 2007). Because, KSR functions exclusively at the plasma membrane, the lack of S338 phosphorylation on Golgi-localized Raf may be explained by the absence of an equivalent Golgi scaffold for CK2. By analogy, Sef, an ERK scaffold protein localized to the Golgi (Torii *et al.*, 2004), may supply alternative Raf-1–activating components, ensuring differential modes of Raf activation. A more limited set of Raf activation mechanisms at the Golgi may be critical to ensure analog MAPK output; in contrast to the plasma membrane where multiple, redundant activation mechanisms are required to match nanocluster lifetime to MAPK module activation (Tian *et al.*, 2007). Consistent with this hypothesis, the dynamics of Ras activation on the Golgi are also much slower than on the plasma membrane (Chiu *et al.*, 2002; Rocks *et al.*, 2005).

Two caveats need to be considered here: First, work from other groups has shown that constitutively active oncogenic mutant Ras targeted to the ER with the same IBVM anchor that we used to target Raf can activate ERK (Chiu *et al.*, 2002; Matallanas *et al.*, 2006), although less efficiently than it activates JNK (Chiu *et al.*, 2002). Our initial study was in BHK cells, but we also observed no activation of MAPK by Raf-IBVM in the NIH3T3 and COS-1 cell lines used for the Ras-IBVM studies; thus cell type differences do not account for our apparently quite different results. The simplest explanation for this discordance is that overexpressed oncogenic Ras is able to recruit additional signaling components or generate additional signals in trans, which allow some degree of kinase activation when Raf is recruited by Ras, whereas these signals are absent when Raf is targeted directly to the ER. We and others concur, however, that MAPK activation does occur on the Golgi, which is the more physiologically relevant endomembrane-signaling compartment (Chiu *et al.*, 2002; Matallanas *et al.*, 2006). Second, although our study makes extensive use of ectopic expression systems with all their inherent limitations, biological relevance is maintained by limiting the extent of over expression and by assaying endogenous MAPK signaling.

Our results indicate that to drive PC12 differentiation, high levels of nuclear ERKpp are necessary. Intriguingly, it appears there are at least two distinct signaling compartments within the Golgi. The first, represented by Golgi-localized CTH-181S, is able to activate the MAPK module to direct PC-12 differentiation. The second Golgi microenvironment corresponds to KDELR, is also able to activate the MAPK module but does not direct PC-12 differentiation. Our data, together with previous findings, indicates that spatial regulation of ERK signaling from the Golgi has a range of biological consequences. Sef has been shown to regulate ERK from the Golgi by inhibiting its nuclear translocation without disrupting its cytoplasmic function (Torii *et al.*, 2004). In addition, another study has shown negative regulation of Raf-1 at the Golgi by an interaction with the protein Raf Kinase Trapping to Golgi (RKTG; Feng *et al.*, 2007). The role of these proteins and precise mechanisms behind how the Golgi regulates positive and negative signaling requires further investigation.

The paradigm of Ras signaling from endomembranes was recently confirmed in fission yeast, where Ras activation at the plasma membrane regulates the MKK Byr2 to control mating, whereas at the endomembrane Ras regulates the Cdc42 exchange factor Scd1 to control cell morphology (Onken *et al.*, 2006). The striking observation that divergent cell fate decisions correspond to differences in Ras localization and ERK activation in T-cells during thymic selection provides indirect but compelling evidence that MAPK system output is also significantly different from the endomembrane compared with the plasma membrane (Daniels *et al.*, 2006). Here we validate these findings by formally showing that different system outputs are indeed generated from plasma membrane versus Golgi-localized Raf.

How cells translate the different signaling kinetics and system outputs from Golgi and plasma membrane MAPK activation into distinct cell fates needs further investigation. It is clear, however, that a high-fidelity measurement of signal strength with a wide dynamic range is provided by ERKpp output from plasma membrane nanoclusters, and it is high-strength signals from this platform immediately after ligand engagement that drives negative selection of T-cells in the thymus. In contrast positive T-cell selection correlates with Golgi-mediated ERK activation occurring at later time points after ligand engagement (Daniels *et al.*, 2006). One additional interesting feature of the signal outputs we observed from the plasma membrane and Golgi is the ability of the Golgi platform to generate delayed but high-strength ERKpp signals in response to low-strength EGF inputs that evoke an initial low-strength ERKpp output from the plasma membrane (Figure 5). Thus although the Golgi reads out the EGF signal with low fidelity (i.e., there is poor correlation between the EGF input and ERKpp output), it opens up a window where a low-strength signal can generate a weak early ERKpp signal, but a strong delayed ERKpp signal. It is tempting to speculate that this system engineering underlies the different cell fates observed for thymic T-cells (Daniels *et al.*, 2006) and, in other cellular contexts, may be used more

widely to link spatial temporal regulation of ERK activation with divergent cell fates.

In summary, our data formally demonstrate the important principle that activation of the same pathway from spatially distinct membrane environments generates different biological outcomes. We show that different environments confer digital versus analog signaling adding another layer of regulation over MAP activation via both lateral segregation on the plasma membrane and subcellular compartmentalization. Importantly, our data reveal Raf activation as the central control point in activating the MAPK module and shows that the different nanoscale environments available to Ras can generate fundamentally different circuit configurations for the MAPK module.

ACKNOWLEDGMENTS

This work was supported by grants from the National Health and Medical Research Council, Australian Research Council (ARC), and the National Institutes of Health GM066717, GM055279, CA116034. Confocal microscopy was performed at the Australian Cancer Research Foundation (ACRF), Institute for Molecular Bioscience (IMB) Dynamic Imaging Facility for Cancer Biology, which was established with the support of the ACRF. The IMB is a Special Research Centre of the ARC.

REFERENCES

Abankwa, D., Hanzal-Bayer, M., Ariotti, N., Plowman, S. J., Gorfe, A. A., Parton, R. G., McCammon, J. A., and Hancock, J. F. (2008). A novel switch region regulates H-ras membrane orientation and signal output. EMBO J. *27*, 727–735.

Apolloni, A., Prior, I. A., Lindsay, M., Parton, R. G., and Hancock, J. F. (2000). H-ras but not K-ras traffics to the plasma membrane through the exocytic pathway. Mol. Cell. Biol. *20*, 2475–2487.

Bivona, T. G., Perez De Castro, I., Ahearn, I. M., Grana, T. M., Chiu, V. K., Lockyer, P. J., Cullen, P. J., Pellicer, A., Cox, A. D., and Philips, M. R. (2003). Phospholipase Cgamma activates Ras on the Golgi apparatus by means of RasGRP1. Nature *424*, 694–698.

Brunet, A., Roux, D., Lenormand, P., Dowd, S., Keyse, S., and Pouyssegur, J. (1999). Nuclear translocation of p42/p44 mitogen-activated protein kinase is required for growth factor-induced gene expression and cell cycle entry. EMBO J. *18*, 664–674.

Chiu, V. K., Bivona, T., Hach, A., Sajous, J. B., Silletti, J., Wiener, H., Johnson, R. L., 2nd, Cox, A. D., and Philips, M. R. (2002). Ras signalling on the endoplasmic reticulum and the Golgi. Nat. Cell Biol. *4*, 343–350.

Choy, E., Chiu, V. K., Silletti, J., Feoktistov, M., Morimoto, T., Michaelson, D., Ivanov, I. E., and Philips, M. R. (1999). Endomembrane trafficking of ras: the CAAX motif targets proteins to the ER and Golgi. Cell *98*, 69–80.

Daniels, M. A., Teixeiro, E., Gill, J., Hausmann, B., Roubaty, D., Holmberg, K., Werlen, G., Hollander, G. A., Gascoigne, N. R., and Palmer, E. (2006). Thymic selection threshold defined by compartmentalization of Ras/MAPK signalling. Nature *444*, 724–729.

Dhillon, A. S., and Kolch, W. (2002). Untying the regulation of the Raf-1 kinase. Arch. Biochem. Biophys. *404*, 3–9.

Diaz, B., Barnard, D., Filson, A., MacDonald, S., King, A., and Marshall, M. (1997). Phosphorylation of Raf-1 serine 338-serine 339 is an essential regulatory event for Ras-dependent activation and biological signaling. Mol. Cell. Biol. *17*, 4509–4516.

Feng, L., Xie, X., Ding, Q., Luo, X., He, J., Fan, F., Liu, W., Wang, Z., and Chen, Y. (2007). Spatial regulation of Raf kinase signaling by RKTG. Proc. Natl. Acad. Sci. USA *104*, 14348–14353.

Goodwin, J. S., Drake, K. R., Rogers, C., Wright, L., Lippincott-Schwartz, J., Philips, M. R., and Kenworthy, A. K. (2005). Depalmitoylated Ras traffics to and from the Golgi complex via a nonvesicular pathway. J. Cell Biol. *170*, 261–272.

Hancock, J. F., Magee, A. I., Childs, J. E., and Marshall, C. J. (1989). All ras proteins are polyisoprenylated but only some are palmitoylated. Cell *57*, 1167–1177.

Hancock, J. F., and Parton, R. G. (2005). Ras plasma membrane signalling platforms. Biochem. J. *389*, 1–11.

Hancock, J. F., Paterson, H., and Marshall, C. J. (1990). A polybasic domain or palmitoylation is required in addition to the CAAX motif to localize p21ras to the plasma membrane. Cell *63*, 133–139.

Harding, A., and Hancock, J. F. (2008a). Ras nanoclusters: combining digital and analog signaling. Cell Cycle *7*, 127–134.

Harding, A., Hsu, V., Kornfeld, K., and Hancock, J. F. (2003). Identification of residues and domains of Raf important for function in vivo and in vitro. J. Biol. Chem. *278*, 45519–45527.

Harding, A., Tian, T., Westbury, E., Frische, E., and Hancock, J. F. (2005). Subcellular localization determines MAP kinase signal output. Curr. Biol. *15*, 869–873.

Harding, A. S., and Hancock, J. F. (2008b). Using plasma membrane nanoclusters to build better signaling circuits. Trends Cell Biol. *18*, 364–371.

Hibino, K., Watanabe, T. M., Kozuka, J., Iwane, A. H., Okada, T., Kataoka, T., Yanagida, T., and Sako, Y. (2003). Single- and multiple-molecule dynamics of the signaling from H-Ras to cRaf-1 visualized on the plasma membrane of living cells. Chem. Phys. Chem. *4*, 748–753.

Jaumot, M., Yan, J., Clyde-Smith, J., Sluimer, J., and Hancock, J. F. (2002). The linker domain of the Ha-Ras hypervariable region regulates interactions with exchange factors, Raf-1 and phosphoinositide 3-kinase. J. Biol. Chem. *277*, 272–278.

Laude, A. J., and Prior, I. A. (2008). Palmitoylation and localisation of RAS isoforms are modulated by the hypervariable linker domain. J. Cell Sci. *121*, 421–427.

Marshall, C. J. (1996). Ras effectors. Curr. Opin. Cell Biol. *8*, 197–204.

Matallanas, D., Sanz-Moreno, V., Arozarena, I., Calvo, F., Agudo-Ibanez, L., Santos, E., Berciano, M. T., and Crespo, P. (2006). Distinct utilization of effectors and biological outcomes resulting from site-specific Ras activation: Ras functions in lipid rafts and Golgi complex are dispensable for proliferation and transformation. Mol. Cell. Biol. *26*, 100–116.

McKay, M. M., and Morrison, D. K. (2007). Integrating signals from RTKs to ERK/MAPK. Oncogene *26*, 3113–3121.

Morrison, D. K., and Cutler, R. E. (1997). The complexity of Raf-1 regulation. Curr. Opin. Cell Biol. *9*, 174–179.

Murakoshi, H., Iino, R., Kobayashi, T., Fujiwara, T., Ohshima, C., Yoshimura, A., and Kusumi, A. (2004). Single-molecule imaging analysis of Ras activation in living cells. Proc. Natl. Acad. Sci. USA *101*, 7317–7322.

Onken, B., Wiener, H., Philips, M. R., and Chang, E. C. (2006). Compartmentalized signaling of Ras in fission yeast. Proc. Natl. Acad. Sci. USA *103*, 9045–9050.

Perez de Castro, I., Bivona, T. G., Philips, M. R., and Pellicer, A. (2004). Ras activation in Jurkat T cells following low-grade stimulation of the T-cell receptor is specific to N-Ras and occurs only on the Golgi apparatus. Mol. Cell. Biol. *24*, 3485–3496.

Plowman, S. J., Ariotti, N., Goodall, A., Parton, R. G., and Hancock, J. F. (2008). Electrostatic interactions positively regulate K-Ras nanocluster formation and function. Mol. Cell. Biol. *28*, 4377–4385.

Plowman, S. J., Muncke, C., Parton, R. G., and Hancock, J. F. (2005). H-ras, K-ras, and inner plasma membrane raft proteins operate in nanoclusters with differential dependence on the actin cytoskeleton. Proc. Natl. Acad. Sci. USA *102*, 15500–15505.

Prior, I. A., Harding, A., Yan, J., Sluimer, J., Parton, R. G., and Hancock, J. F. (2001). GTP-dependent segregation of H-ras from lipid rafts is required for biological activity. Nat. Cell Biol. *3*, 368–375.

Prior, I. A., Muncke, C., Parton, R. G., and Hancock, J. F. (2003). Direct visualization of Ras proteins in spatially distinct cell surface microdomains. J. Cell Biol. *160*, 165–170.

Ritt, D. A., Zhou, M., Conrads, T. P., Veenstra, T. D., Copeland, T. D., and Morrison, D. K. (2007). CK2 Is a component of the KSR1 scaffold complex that contributes to Raf kinase activation. Curr. Biol. *17*, 179–184.

Robinson, M. J., Stippec, S. A., Goldsmith, E., White, M. A., and Cobb, M. H. (1998). A constitutively active and nuclear form of the MAP kinase ERK2 is sufficient for neurite outgrowth and cell transformation. Curr. Biol. *8*, 1141–1150.

Rocks, O., Peyker, A., Kahms, M., Verveer, P. J., Koerner, C., Lumbierres, M., Kuhlmann, J., Waldmann, H., Wittinghofer, A., and Bastiaens, P. I. (2005). An acylation cycle regulates localization and activity of palmitoylated Ras isoforms. Science *307*, 1746–1752.

Roy, S., Lane, A., Yan, J., McPherson, R., and Hancock, J. F. (1997). Activity of plasma membrane-recruited Raf-1 is regulated by Ras via the Raf zinc finger. J. Biol. Chem. *272*, 20139–20145.

Roy, S., Plowman, S., Rotblat, B., Prior, I. A., Muncke, C., Grainger, S., Parton, R. G., Henis, Y. I., Kloog, Y., and Hancock, J. F. (2005). Individual palmitoyl residues serve distinct roles in H-ras trafficking, microlocalization, and signaling. Mol. Cell. Biol. *25*, 6722–6733.

Roy, S., Wyse, B., and Hancock, J. F. (2002). H-Ras signaling and K-Ras signaling are differentially dependent on endocytosis. Mol. Cell. Biol. *22*, 5128–5140.

Santos, S. D., Verveer, P. J., and Bastiaens, P. I. (2007). Growth factor-induced MAPK network topology shapes Erk response determining PC-12 cell fate. Nat. Cell Biol. *9*, 324–330.

Tian, T., Harding, A., Inder, K., Plowman, S., Parton, R. G., and Hancock, J. F. (2007). Plasma membrane nanoswitches generate high-fidelity Ras signal transduction. Nat. Cell Biol. *9*, 905–914.

Tohgo, A., Pierce, K. L., Choy, E. W., Lefkowitz, R. J., and Luttrell, L. M. (2002). beta-Arrestin scaffolding of the ERK cascade enhances cytosolic ERK activity but inhibits ERK-mediated transcription following angiotensin AT1a receptor stimulation. J. Biol. Chem. *277*, 9429–9436.

Torii, S., Kusakabe, M., Yamamoto, T., Maekawa, M., and Nishida, E. (2004). Sef is a spatial regulator for Ras/MAP kinase signaling. Dev. Cell *7*, 33–44.

Traverse, S., Gomez, N., Paterson, H., Marshall, C., and Cohen, P. (1992). Sustained activation of the mitogen-activated protein (MAP) kinase cascade may be required for differentiation of PC12 cells. Comparison of the effects of nerve growth factor and epidermal growth factor. Biochem. J. *288*(Pt 2), 351–355.